Contemporary Changes in the Geoid About Greenland: Predictions Relevant to Gravity Space Missions

Kevin Fleming, Zdeněk Martinec, Jan Hagedoorn, and Detlef Wolf

GeoForschungsZentrum Potsdam, Dept. Geodesy and Remote Sensing, Potsdam, Germany, *kevin@gfz-potsdam.de*

Summary. We have examined contemporary changes in the geoid about Greenland that result from glacial-isostatic adjustment. These may be divided into contributions from ice-load changes that occurred outside of Greenland following the Last Glacial Maximum and changes in the Greenland Ice Sheet (GIS). The GIS's contribution may itself be divided into past and current parts. For past ice-load changes, the resulting geoid displacement is more dependent upon the recent history of the GIS than on the earth model used. Considering an estimated accuracy for the GRACE temporal geoid signal, regional variability in the present-day mass balance of the GIS may be resolved. This variability significantly affects the geoid power spectrum, giving a signal that may be detected by measurements from gravity space missions more easily than has been proposed by other authors.

Key words: Geoid change, CHAMP and GRACE satellite missions, glacial-isostatic adjustment, Greenland Ice Sheet.

1 Introduction

The mass balance of the global continental ice cover, particularly the ice sheets of Antarctica and Greenland, is a crucial element when determining present-day sea-level change. However, because of the size and inaccessibility of these ice masses, such knowledge is currently lacking in detail.

Alternatively, information about the mass balance of these ice sheets may be gained by resolving temporal and spatial changes in the *geoid*, *i.e.* the equipotential surface of the Earth's gravity field that approximates mean sea level. These changes arise from the redistribution of mass within the Earth and upon its surface, in particular from the waxing and waning of ice sheets during glacial cycles.

We have assessed the contemporary geoid change about Greenland resulting from past changes in the major ice sheets and the current behaviour of the Greenland Ice Sheet (GIS). This is examined within the context of the gravity space missions now underway (CHAMP and GRACE).

2 Contribution of ongoing GIA

We first assess geoid change arising from ongoing glacial-isostatic adjustment (GIA) due to changes in ice loading following the Last Glacial Maximum (LGM, *ca.* 21 ka BP). We apply a gravitationally self-consistent GIA model based on the spectral finite-element method (1). The sea-level equation is also implemented and accommodates changes in the Earth's rotation, moving shorelines and the transition between grounded and floating ice.

A four-layer earth model is used, described by the elastic-lithosphere thickness, h_{L}, the upper-mantle viscosity, η_{UM}, the lower mantle-viscosity, η_{LM}, and an inviscid core. The mantle is an incompressible, Maxwell-viscoelastic fluid and the mass-density and elastic shear-modulus values are from PREM. Two viscosity models are used: EARTH1, similar to that preferred by (2), and EARTH2, similar to that used by (3).

The ice models are the global ice model ICE-3G (4) without its Greenland component (termed ICE-3G–GR), the Greenland ice model GREEN1 (5), which accommodates changes in the GIS since the LGM, but excludes a neoglacial component (when the GIS had retreated behind its present-day margin and readvanced over the past *ca.* 4 ka), and GREEN1+NEO, which is GREEN1 including neoglaciation in the southwest.

Fig. 1 presents the resulting spectra (where spectrum refers to the square root of the degree-power spectrum) from the individual ice and earth model combinations. We find there is a relatively small dependence on the viscosity model used. In contrast, the inclusion or exclusion of the neoglacial component is more important to Greenland's predicted contribution. This is further shown in Fig. 2, where the rates of uplift and geoid change are presented. Again, the neoglaciation is more significant, especially for the EARTH1 model, owing to the more-rapid reaction of its lower upper-mantle viscosity.

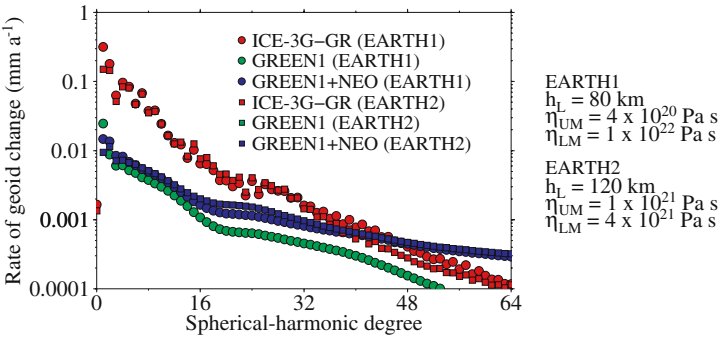

Fig. 1. The geoid-change spectra resulting from the deglaciation following the LGM.

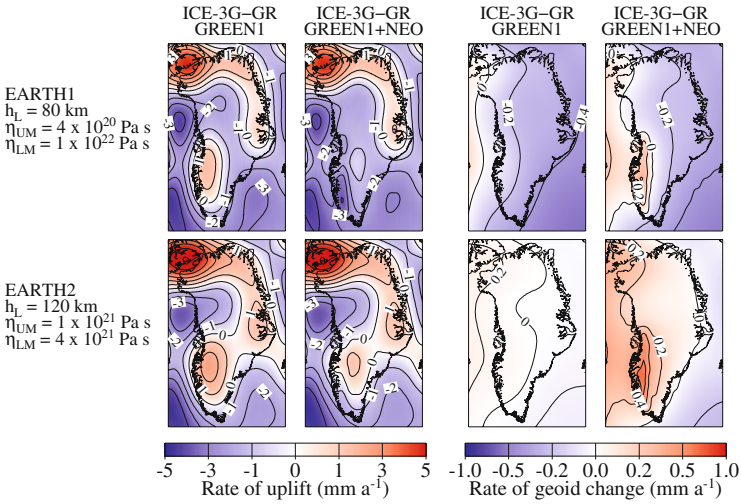

Fig. 2. The present-day rates of uplift and geoid change resulting from the deglaciation following the LGM.

3 Present-day changes in the GIS

Two estimates of the current mass balance of the GIS are examined (Fig. 3). The first, KRABILL (Fig. 3a) (6), is based on airborne laser-altimeter measurements of changes in ice-surface elevation and covers the entire ice sheet. We have corrected the changes in ice-surface elevation for ongoing GIA using results for EARTH1 and ICE-3G–GR+GREEN1+NEO. These corrections are usually relatively small, especially when one considers the measured changes along the ice margin.

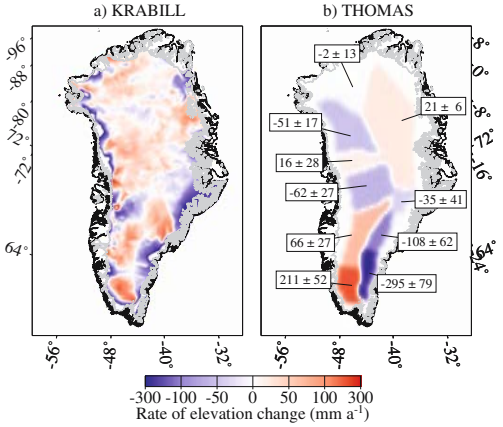

Fig. 3. The mass-balance models of the GIS used in this study. (a) KRABILL considers the entire GIS, (b) while THOMAS covers the area above *ca.* 2000 m.

The second estimate, THOMAS (Fig. 3b) (7), is based on GPS measurements and ice-flow calculations. It represents the mass balance above *ca.* 2000 m elevation. Its equivalent sea-level contribution (*ca.* 0.015 mm a^{-1}) is opposite in sign to the KRABILL value (*ca.* –0.033 mm a^{-1}) for the same area.

4 GIS-induced geoid change

We compare the spectra corresponding to the Greenland mass-balance scenarios (Fig. 4a) and the associated geoid changes (Fig. 4b). Three series of results for KRABILL are presented: (a) the entire ice sheet, (b) the area corresponding to THOMAS (above *ca.* 2000 m elevation) and (c) the area excluded by THOMAS (below *ca.* 2000 m elevation). Spectra for THOMAS are calculated for all combinations of the uncertainties about the nominal values.

Changes below 2000 m elevation dominate the KRABILL results. We also note that the upper limit of the range of the THOMAS results is comparable to the total KRABIL response. Some spatial variability in the rate of geoid change can be seen when the spectra are summed up to degree and order 32 (Fig. 5). The opposite signs of the equivalent sea-level contributions for THOMAS and KRABILL (>2000 m) are also apparent (Fig. 5c and d).

5 Discussion and summary

Some investigators have assumed uniform ice-mass changes when calculating geoid signals (8). We have examined this assumption using versions of KRABILL and THOMAS where the net ice-volume changes are uniformly distributed over the respective areas. The resulting geoid-change spectra (Fig. 6) fall off more quickly with increasing degree than those for more realistic spatial distributions.

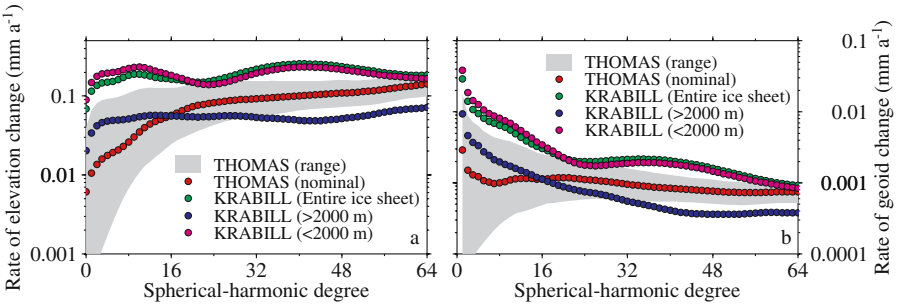

Fig. 4. (a) The mass-balance spectra (Fig. 2) and (b) the resulting geoid-change spectra.

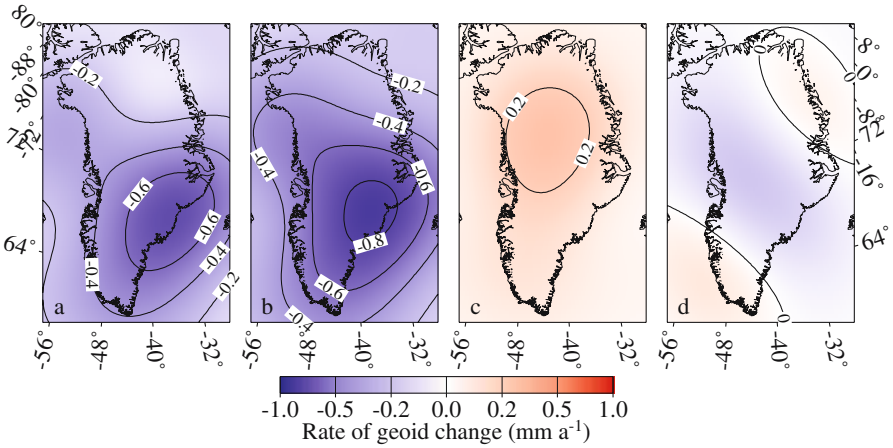

Fig. 5. Rates of geoid change for the various mass-balance scenarios: (a) KRABILL (entire GIS), (b) KRABILL (below *ca.* 2000 m elevation), (c) KRABILL (above *ca.* 2000 m elevation) and (d) THOMAS.

Finally, we compare the predicted spectra with an accuracy estimate for GRACE (Fig. 7). The total ongoing-GIA response is largest at lower degrees, but falls off quickly. The GIS signal, specifically for KRABILL, remains above the uncertainty up to degree *ca.* 64, but the signal for THOMAS is of similar magnitude. We also find that, while the geoid-change signal for Antarctica's present-day ice-mass balance (9) is much greater than for Greenland's, it has a similar shape.

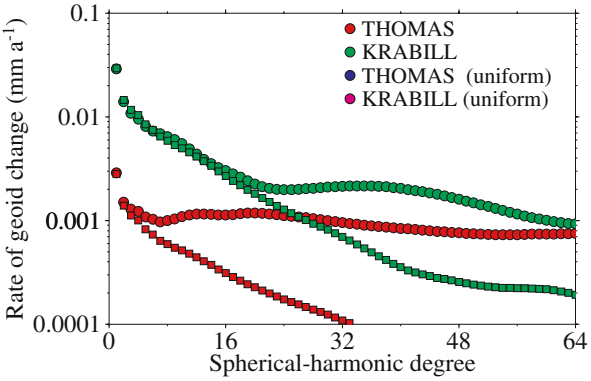

Fig. 6. The geoid-change spectra for the KRABILL and THOMAS mass-balance scenarios for realistic and uniform spatial descriptions.

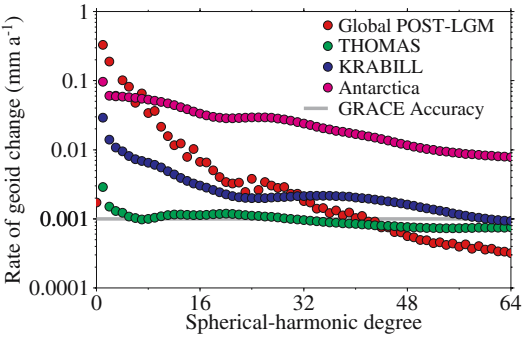

Fig. 7. The geoid-change spectra for the various models discussed in this study, and for an estimate of the present-day ice-mass changes in Antarctica. An estimate of the accuracy expected from the GRACE satellite mission is included.

Acknowledgement. This study was supported by the SEAL (Sea Level Change) project of the Hermann von Helmholtz Association of German Research Centres.

References

[1] Martinec Z (2004) Time-domain, spectral-finite element method to viscoelastic relaxation of a self-gravitating, incompressible, Maxwell-viscoelastic, radially symmetric sphere. Computers and Geosciences, submitted.

[2] Lambeck K, Smither C and Ekman M (1998) Tests of glacial rebound models for Fennoscandinavia based on instrumented sea- and lake-level records. Geophys J Int *135*: 375–387.

[3] Mitrovica JX and Peltier WR (1989) Pleistocene deglaciation and the global gravity field. J Geophys Res *94*: 13,651–13,671.

[4] Tushingham AM and Peltier WR (1998) Ice 3G: a new global model of late Pleistocene deglaciation based on geophysical predictions of postglacial relative sea level change. J Geophys Res *96*: 4,497–4,523.

[5] Fleming K and Lambeck K (2004) Constraints on the Greenland Ice Sheet since the Last Glacial Maximum from sea-level observations and glacial rebound models. Quat Sci Rev, in press.

[6] Krabill W, Abdalati W, Frederick E, Manizade S, Martin C, Sonntag J, Swift R, Thomas R, Wright W and Yungel J (2000) Greenland Ice Sheet: high-elevation balance and peripheral thinning. Science *289*: 428–430.

[7] Thomas R, Akins T, Csatho B, Fahnestock M, Gogineni P, Kim C and Sonntag J (2000) Mass balance of the Greenland Ice Sheet at high elevations. Science *289*: 426–428.

[8] Velicogna I and Wahr J (2002) Postglacial rebound and Earth's viscosity structure from GRACE. J Geophys Res *107*: 2,376–2,387.

[9] Rignot E and Thomas R (2002) Mass balance of polar ice sheets. Science *297*: 1,502–1,506.